Antibody Affinity Maturation to SARS-CoV-2 Omicron Variants in a Teachers Cohort

Philip H. James-Pemberton[1,] Shivali Kohli, Aaron C. Westlake, Alex Antill, Rouslan V. Olkhov and Andrew M. Shaw[1,2*]

[1]Biosciences, University of Exeter, Stocker Road, Exeter, EX4 4QD, UK

[2]Attomarker Ltd, 3 Babbage Way, Exeter Science Park, Exeter, Devon, EX5 2FN, UK

Abstract

In summer of 2022, a cohort of 28 staff members were recruited from a UK primary school setting. The prevalent variants at the time were Omicron BA.1.159, BA.4/5 and BA.2: 61% of the cohort reported a lateral flow confirmed positive test for SARS-CoV-2 infection in late 2021 or 2022. A fully quantitative antibody screen for concentration and affinity was performed for spike protein variants Wuhan, Alpha, Beta, Gamma, Delta and Omicron BA.1, BA.2.75, BA.2.12.1, BA.4 and BA.5 and a pH dependent affinity was derived from disruption of the epitope-paratope complex at pH 3.2. The cohort showed a Universal positive immunity endotype, U(+), incidence of 78% (95% CI 60% - 88%) with good antibody concentrations to all ten variants; the incidence drops to 25% (95% CI 13% - 43%) when the affinity spectrum is measured. The antibody affinity profiles for each Omicron variant were all significantly better than Alpha, Beta, Gamma and Delta reflecting exposure to the antigens; we surmise either from the booster vaccines or continual contact with the virus, presenting in the school children either asymptomatically or symptomatically. Significant antibody affinity maturation was seen to the spike protein in all prevalent variants of SARS-CoV-2. Antibody concentrations were waning compared to the post-booster vaccine response. Using our hypothesised 3.4 mg/L nasal mucosal protection threshold, we postulate 46% of the cohort required boosting within 60 days and 66% within 120 days. We propose a smart boosting programme around the constant-exposure teacher cohort and parents of children could reduce community transmission.

Funding – Exeter University Alumni, Attomarker Ltd funded PhD studentship at the University of Exeter and Attomarker Ltd funding directly.

Introduction

School staff members are uniquely exposed to transient infections in children when in enclosed, poorly ventilated environments, including during the SARS CoV-2 pandemic[1]. A recent retrospective test-and-trace study from Italy[2] has shown that, of the school students in the age range 6 -10 years, 50% (95% CI, 39% - 60 %) tested positive and were asymptomatic carriers and 21.4% (95% CI 14% – 31%) had symptomatic infections for SARS CoV-2. Similarly, studies in the UK following the release of school teaching restrictions showed a surge in student infections during the period August to October 2021[3] with household clusters adding to transmissions in parents, particularly from children aged 5-15. Other studies counter with findings that school children in the pandemic[4] in the age range 5–11 years old did not have a prevalence of infection greater than the local working population, although it is noteworthy that the prevalence of asymptomatic carriers was not reported.

We assume herein, that the immune system of teachers is constantly challenged by the presence of infections such as SARS-CoV-2 and others throughout the year. For some teachers, repeated or constant exposure could maintain antibody and T cell levels optimised against the prevailing variants, and so this constant-exposure cohort may develop or evolve immunity to the virus. In a recent study elsewhere[5], we observe a number of new immunity endotypes that show universal protection against the variants Wuhan, Alpha, Beta, Gamma, Delta and Omicron (BA.1) with a prevalence of up to 75% of the population. The universal protection is consistent with raising antibodies to epitopes that are present in all variants in regions other than the receptor binding domain, such as the hinge region required for the S protein to transition from pre-fusion to fusion state. Meanwhile, immunity endotypes of the remaining 25% show poor antibody production or drop-outs to one or more of the variants due to having made antibodies to epitopes that are not present in all variants. The drop-out endotypes may be imprinted in some teachers and repeated exposure, such as that in a school environment could result in poor immunity against the prevailing variants and cause recurrent sickness. For some drop-out endotypes, repeated exposure may also trigger the memory production of low affinity antibodies (and potentially T cells) that are present in high levels but ineffective, explaining why some members of the population appear to be vulnerable to repeat infections despite comparatively high antibody levels to some measured variants. There remains a possibility however, that a constant exposure environment may refine the imprint in favour of more optimised epitopes with better antibody affinity.

Immunity endotypes were previously explored for the concentration of antibodies against variant spike proteins[5] but affinity of the antibody-antigen interactions is also an important and potentially evolving immunity endotype. Measurement of antibody affinity (or avidity) requires the dissociation rate of the paratope-epitopes complex to be accurately measured, and for stable complexes this may correspond to a half-life of several hours. Further, the stability of the complex in serum may be a poor mimic of the mucosal environment where the pH may be more acidic, pH 5.5. We have explored a

new method of assessing the stability of the paratope-epitope complex by measuring a ratio between antibody-antigen binding responses at two different pH values: pH 3.2 and pH 7.4. The product of the binding ratio for pH-dependent affinity and the total concentration of antibodies then provides a measure of vaccine efficiency against all spike variant proteins.

In this paper, we report a prospective cohort study on 28 staff members in a primary school setting with samples taken 13th July 2022. The local prevalent Omicron variants at the time of sampling were BA.4 and BA.5, whilst BA.1.1 and BA.2 were prevalent in the preceding 6 months. Demographic data was collected alongside vaccination histories and lateral flow confirmations of any recent infections. A COVID antibody immunity test was performed for nucleocapsid, Spike (Wuhan), Spike Omicron BA.1 and receptor binding domain. A further concentration and pH-dependent affinity profile was collected for the spike proteins for the variants Wuhan, Alpha, Beta, Gamma, Delta, as well as Omicron sub-variant strains BA.1, BA.2.75, BA.2.12.1, BA.4 and BA.5. The full 20-dimensional profile of concentration and pH-dependent affinity for 10 variants for each adult tested in the school was interpreted in the constant-exposure cohort context.

Materials and Methods

Materials

Materials used throughout the course of the experiments were used as supplied by the manufacturer, without further purification. Sigma-Aldrich supplied phosphate buffered saline (PBS) in tablet form (Sigma, P4417), phosphoric acid solution (85 ± 1 wt. % in water, Sigma, 345245) and Tween 20 (Sigma, P1379). Glycine (analytical grade, G/0800/48) was provided by Fisher Scientific. Assay running and dilution buffer was PBS with 0.005 v/v % Tween 20 and the regeneration buffer was 0.1 M phosphoric acid with 0.02 M glycine solution in deionized water.

A recombinant human antibody to the spike protein S2 subdomain, a chimeric monoclonal antibody (SinoBiological, 40590-D001, Lot HA14AP2901) was used as a calibrant. The antibody was raised against recombinant SARS-CoV-2 / 2019-nCoV Spike S2 ECD protein (SinoBiological, 40590-V08B). This was selected as it could bind to all nine Spike protein variants used herein.

NISTmAb, a recombinant humanized IgG1κ with a known sequence[6] specific to the respiratory syncytial virus protein F (RSVF)[7], was from National Institute of Standards and Technology (RM8671). The detection mixture consisted of a 200-fold dilution of IG8044 R2 from Randox in assay running buffer. The Spike Variant sensor chips were printed as detailed elsewhere [8]. The Omicron sub-variant sensor chips were printed with recombinant human serum albumin from Sigma-Aldrich (A9731), protein A/G from ThermoFisher (21186), and five SARS-CoV-2 Spike Protein variants for the Wuhan, Omicron BA.1, BA.2.12.1, BA.4, BA.5 strains from SinoBiological and BA.2.75 strain from Acro Biosystems as detailed in Table S1.

Methods

Biophotonic Multiplexed Immuno-kinetic assay

The multiplexed biophotonic array platform technology has been described in detail elsewhere[5,8-11] and is now CE marked to perform the Attomarker COVID Antibody Immunity Test. Briefly, the technology is a localised particle plasmon gold sensor which scatters light proportional to the mass of material (formally refractive index) near to the gold nanoparticle surface in the plasmon field. The gold nanoparticles are printed into an array of 170 spots which are then individually functionalised with the protein required. The SARS-CoV-2 antibody targets within the CE marked COVID Antibody immunity Test are nucleocapsid, receptor binding domain, Wuhan spike protein and Omicron spike protein. The inflammation marker C-reactive protein is also measured. The assay consists of a capture step, a detection step and a regeneration step with intervening wash steps. High and low controls are used to calibrate the sensor response and are repeated at regular intervals to ensure quality control[6] during the day..

Two further arrays were fabricated. One containing Spike proteins from SARS-CoV-2 variants, as detailed elsewhere[5], alongside a new array containing the Omicron sub-variants as listed in Table S1. The integrity of the protein samples on the surface was tested using an anti-S2 antibody (40590-D001), chosen for calibration as the corresponding epitope is present on all variants. The concentration of the antibody was calibrated against the NIST antibody RM8671, NISTmAb, a recombinant humanized IgG1κ with a known sequence[6] to assure monomeric purity of the antibody. High-control and low-control samples were made using the 40590-D001 antibody and these controls were then used to quantify results from human samples in units of mg/L. Thus, the assay response is presented as a concentration of an antibody equivalent in its binding properties to the 40590-D001 control antibody. An assay common to each sensor chip was performed using the S (Wuhan) channel, with each array carrying an identical protein. There was high correlation between S channel performance on the two array types (m, c >0.92) and so the results were treated as aligned, Table S2 and Figure S2.

An endotype classification has been derived for the spike protein variant[5] and is shown in Table S2. The endotype classification is based on the instrument characteristics: Limit of Detection (LoD) = 0.2 mg/L and 10 × LoD = Limit of Quantification (LoQ) = 2 mg/L. A full correlation analysis for all combinations of responses was also performed from which the correlation coefficients and lines of best fit were derived. A new measure of antibody affinity has been derived comparing the antibody binding on the surface of the target antigen after a 30 s wash step at either physiological serum pH 7.4 or pH 3.2. The lower pH of 3.2 results in some dissociation of the paratope-epitope complex leading to an effective reduction of the measured antibody concentration; a measurement of the antibodies

that remain strongly bound at pH 3.2 – a high-affinity concentration. A full dissociation occurs at pH 1.9; the pH used at the longer regeneration step. The ratio of these results gives the Antibody Efficiency:

$$\text{Antibody Efficiency} = \frac{\text{concentration(pH 3.2)}}{\text{concentration(pH 7.4)}}$$

The endotype classification can be re-assigned based on the measured high-affinity concentration. The patient demographics and both endotype classifications are shown in Table 1.

Patient Cohort

The staff members were recruited from a primary school setting and took the CE marked Attomarker Antibody Immunity Test after giving informed consent with a registered healthcare professional for the use of their residual blood samples to be used in aiding understanding of the pandemic. The venous blood samples were analysed on site within 7 minutes, and the results subsequently provided to the patients. The residual vacutainer blood was transported back to the laboratory and centrifuged at 1300 rpm for 10 minutes to separate the blood constituents. The serum was collected and subsequently used for variant profile screening.

Ethical Approval

The use of the Attomarker clinical samples was approved by the Bioscience Research Ethics Committee, University of Exeter.

Results

The teacher cohort, *n*=28, recruited from the school was 86% female and 14% male: 68% had an initial AstraZeneca (AZ) two-vaccination dose, 25% Pfizer, 4% Moderna and 4% undeclared, Table 1 (and Table S4). Seven teachers in the cohort or 25 % (95% CI 13% - 43%) were un-boosted. Each teacher had a full concentration and pH-dependent affinity profile assessment for each of the ten spike proteins. A pH-dependent affinity titration for a teacher is shown in Figure S3 for nucleocapsid, Spike protein, Omicron Spike Protein and receptor binding domain. The immunity profile for select patients, showing concentration, high-affinity concentration and antibody efficiency endotypes are shown in Figure 1, with the full classification for the cohort presented in Table 1.

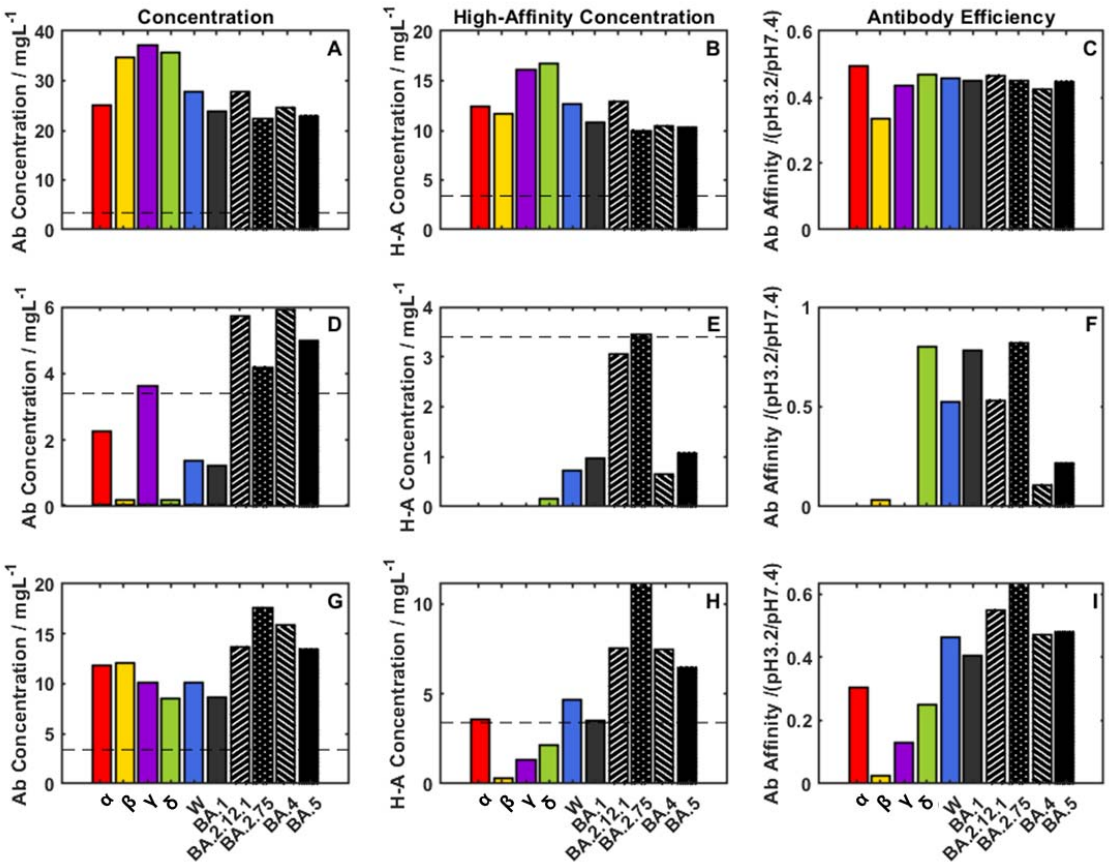

Figure 1 Three samples (one per row) showing 10-variant concentration profiles (A,D,G) column 1, high-affinity concentration profiles (B,E,H) column 2 and Antibody Efficiency profiles (C,F,I) column 3.

The teacher cohort has a confirmed infection incidence in the preceding six months of 61% (95% CI 42% -76%) with a concentration universal endotype, U(+) incidence of 78% (95% CI 60% - 88%) consistent with the incidence observed in our previous study[5], shown in Figure 1(A). Of the remaining six teachers, five showed a Delta drop-out endotype either alone or in combination with Beta: the two Beta drop-out endotypes were associated with a Pfizer vaccination history similar to previous observations[5]. The vaccine efficiency classification, the product of antibody concentration

and pH dependent affinity, shows a more complex picture. The total Universal Efficiency endotype, U(+), incidence falls by a third to 7, or 25% (95% CI 13% - 43%). The drop-out variants (*n*=18 or 64% (95% CI 46% - 79%)) are exclusively early variant drop-outs: none are Omicron variant dropouts.

The cohort bee-swarm box-plots shown in Figure 2 show median concentrations for all variants to be equivalent, but with significantly lower median pH-dependent affinity values (Wilcoxon: Wuhan *vs* Beta $P = 6.1x10^{-8}$, Wuhan *vs* Gamma $P = 5.3x10^{-6}$). The dynamic range of the pH-dependent avidity is 1 – 0.1 and shows discrimination, potentially with bimodal distributions, across the teacher cohort.

Table 1 Cohort demographics including vaccination profile, infection history and endotype classification for concentration and high-affinity concentration (AstraZeneca (AZ), Undeclared (U), U(+) is the universal endotype, variant dropouts α,β,γ,δ,ο and unclassified (UC)) (Sample IDs are not known to the patient)

Sample ID	Interval since recent positive test	Vaccine	Booster	Number of doses	Quantity Endotype	Total Efficiency Endotype
C104	< 4 months	AZ	U	3	U(+)	UC
C105		Pfizer	Pfizer	3	δ (-)	α δ
C106	< 4 months	Pfizer	Pfizer	3	U(+)	β
C107	< 5 months	Pfizer		2	βδ (-)	α β γ δ
C108	< 1 month	AZ	Pfizer	3	U(+)	γ
C109	< 5 months	AZ	Moderna	3	U(+)	UE(+)
C110	< 6 months	Pfizer		2	U(+)	α β γ
C111	< 1 month	AZ	Moderna	3	U(+)	a β g δ
C112		AZ	Moderna	3	U(+)	β
C113	< 1 month	U	U	3	U(+)	UE(+)
C114	< 4 months	Pfizer	Pfizer	3	βδ (-)	α β γ δ
C115	< 5 months	AZ	Pfizer	3	U(+)	UE(+)
C116	< 3 months	AZ	U	2	U(+)	β
C117	< 2 months	AZ	Moderna	3	U(+)	UE(+)
C118		Moderna	Moderna	3	U(+)	β
C119		AZ		2	δ (-)	α β γ δ
C120	< 3 months	Pfizer	Pfizer	3	U(+)	α β γ
C121		AZ	Moderna	3	U(+)	UE(+)
C122	< 3 months	AZ		2	U(+)	β γ
C123		AZ	Pfizer	3	U(+)	α
C124		AZ	Pfizer	3	UC	γ δ
C125		Pfizer		2	U(+)	UE(+)
C126	< 1 month	AZ	Pfizer	3	U(+)	β
C127	< 1 month	AZ	Moderna	3	U(+)	UE(+)
C128	< 4 months	AZ	Moderna	3	U(+)	β
C129		AZ	Moderna	3	U(+)	UC
C130	< 8 months	AZ	Pfizer	3	δ (-)	β γ δ
C131		AZ		2	U(+)	UC

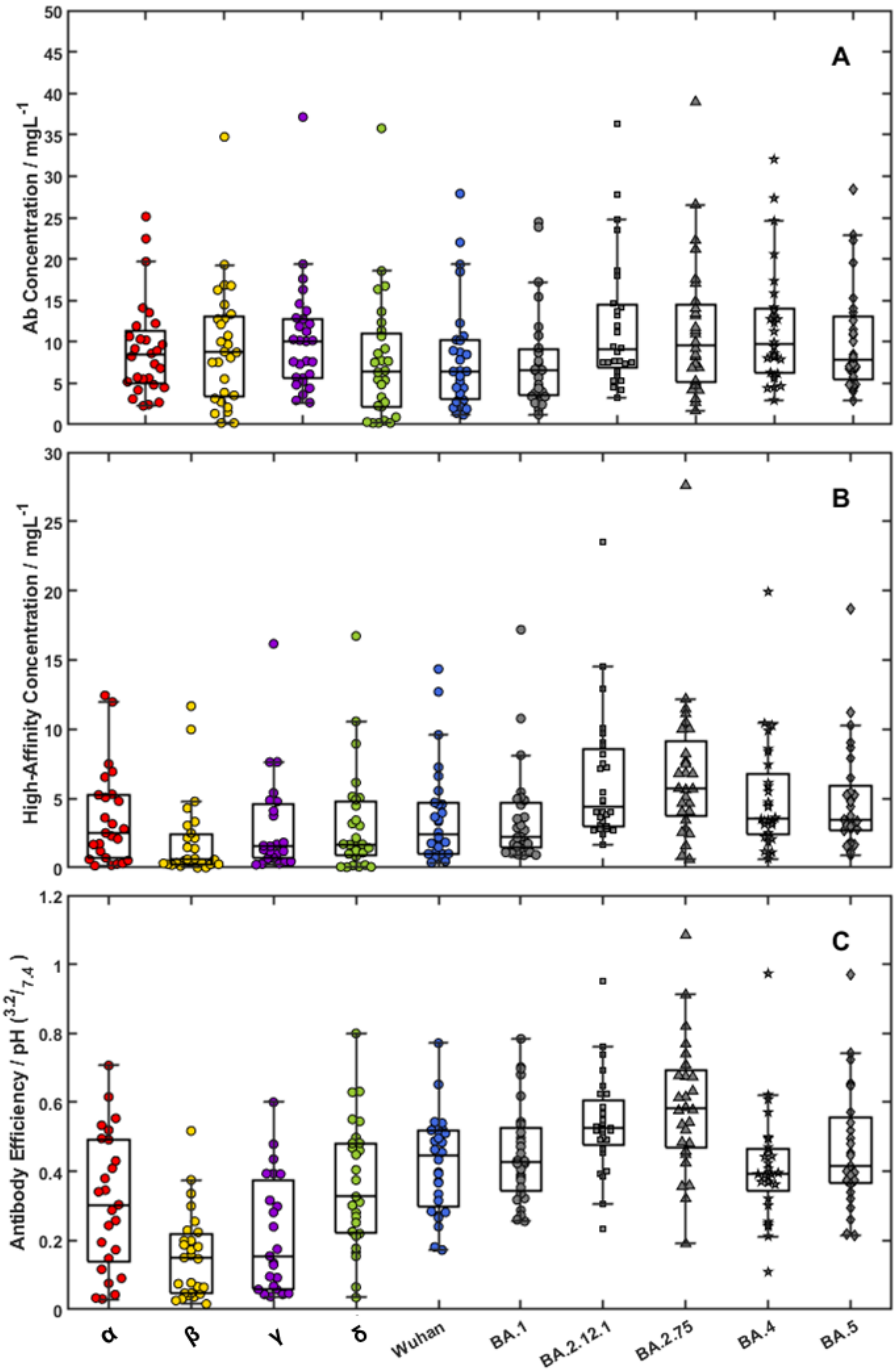

Figure 2 Bee-swarm plot for the Cohort Profiles: (top panel) concentration, (middle panel) high-affinity concentration and Antibody Efficiency (lower panel)

The teacher cohort has Spike and Omicron spike protein antibody distributions shown in Figure 3 indicating 32% (95% CI 18% - 51%) are below the 3.4 mg/L nasal mucosa protection threshold and 36% (95% CI 21% - 54%) are below the Omicron Spike threshold. The concentration distribution of teachers with infection in the last 120 days is shown in red in Figure 3 indicating some super-responders: The two highest results on both plots are from the same samples that had received

boosters during that time period: Sample 1 showed (Wuhan/Omicron) 27/23 mg/L having received a booster in March 2022, and Sample 2 showed 22/25 mg/L having received a booster in May 2022. Of the recently infected individuals, only two are below the 3.4 mg/L threshold following infection.

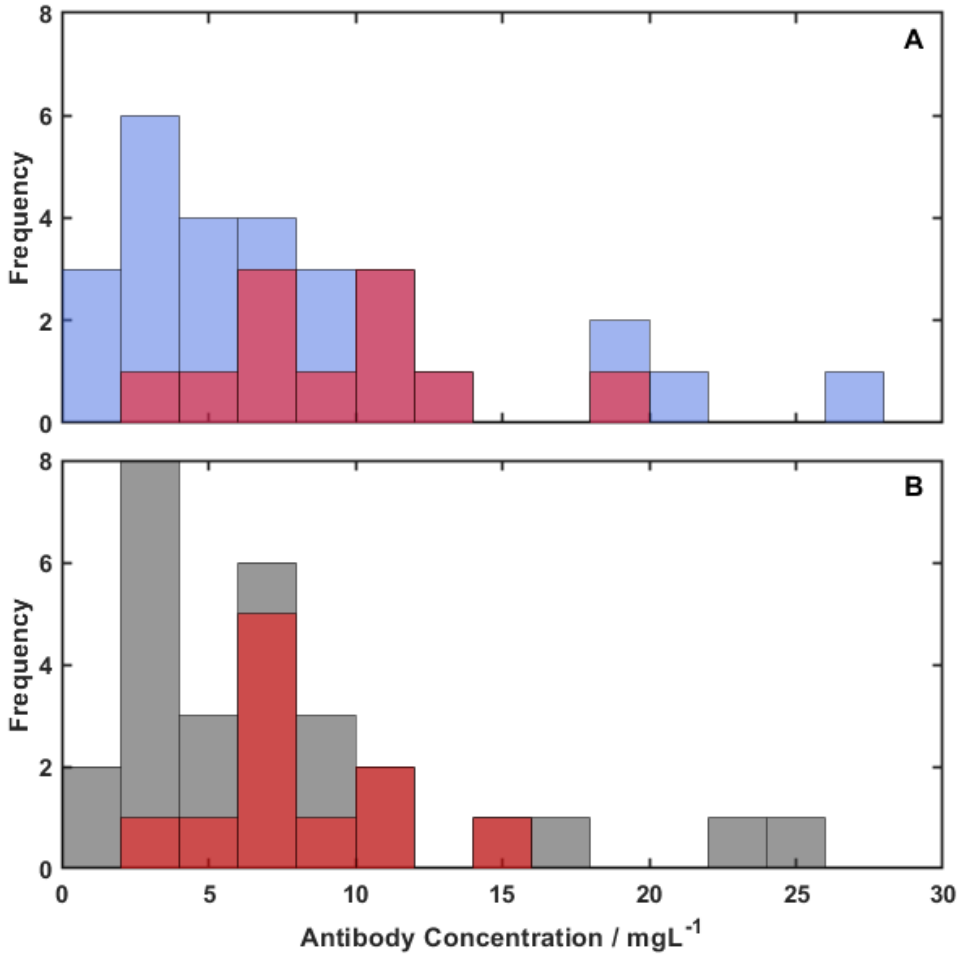

Figure 3 The S (A) and SO (B) protein antibody distributions for the teachers cohort with 67% infection in the preceding six months. The nasal mucosal protection threshold is 3.4 mg/L with 10 teachers below the SO threshold and 9 below the S threshold. Red bars show those with confirmed infection in last 120 days as a subset of each group.

Discussion

The teacher cohort is uniquely exposed in the school setting to children, especially of younger age, that are either virus-positive asymptomatic carriers or symptomatic cases[2,3] in the COVID pandemic, and in the 'new-normal' where repeated waves of infection lead to a high virus prevalence and infection. Schools have been identified[12] as foci of the pandemic although the children themselves may not be vulnerable to infection, leading to difficult discussions about child vaccination[13]. Countries have differed in their approach despite WHO recommendations[14]. The effect of re-opening schools in the UK showed significant increase in infection rates amongst school children[12]. The

teachers and parents of school children represent one of the critical immunity perimeters of the pandemic with consequent implications for workforce sickness and impact on economic activity. The constant-exposure teachers cohort, whether unvaccinated, vaccinated or boosted, are exposed repeatedly to the virus and, if the vaccine provides protection, should have a refined immunity response.

Immunity Imprinting has been reported for SARS-CoV-2 vaccination[15] and we have reported immunity endotypes for antibody concentration against a spectrum of variant spike proteins[5] suggesting that initial exposure to a virus or vaccine may imprint a remembered immune response. Antibody quality or antibody affinity maturation has been reported for SARS-CoV-2 immunity[16,17] with mechanisms of maturation proposed in the germinal centre B cell response[18,19] critical to the adaptive immunity response[20]. Sustained antigen availability has also pointed to non-standard vaccination strategies to optimise this adaptive response[21,22]. The teacher cohort is therefore an ideal setting for the observation of antibody immunity imprinting and consequence maturation.

There is a spectrum of immunity in the teacher cohort derived from vaccination as well as boosted staff (four of whom reported sickness and had time off work), Table 1. The incidence of LFT-confirmed infection in the preceding six months was 63% suggesting exposure to BA.1.159, BA.4/5 and BA.2, Figure 3 and Figure S1. The antibody concentration profile across the spectrum of spike proteins showed the cohort incidence of U(+) was 75% and reflects previous measurements indicating that many had moderate-high antibody levels to all variants, potentially from targeting a universal epitope most likely located on the hinge region of the protein[5]. However, the new measure of antibody quality, pH-dependent affinity, shows significant variation across variants. The Wuhan antibodies generated by the boosted vaccination, and so renewed exposure to the antigen, showed affinity similar to the prevailing variants but was significantly worse for Alpha, Beta and Gamma (Kolmogorov-Smirnov test P values: Alpha=0.016, Beta=$4.1\text{x}10^{-8}$, Gamma=$1.84\text{x}10^{-5}$, Delta=0.28, BA.2.12.1=0.016, BA.2.75=0.0023, BA.4=0.47, BA.5=0.91, BA.1=0.91 *vs* Wuhan). Thus, the U(+) endotype incidence drops to 25%. Figure 1 (A, B, C), shows access to the universal epitope, fully affinity-matured to all variants following vaccine exposure; a highly efficient adaptive response. However, some U(+) endotypes with promising antibody concentration profiles, Figure 1 (G, H, I), do not have antibodies matured against Beta or Gamma variants, leading to lower high-affinity antibody concentration and therefore lower vaccine efficiency against these particular variants. The cohort distributions show a significant antibody maturation and consequent vaccine efficacy towards the Omicron sub-variants (High-Affinity Concentration data Kolmogorov-Smirnov test P values: Alpha=0.47, Beta=0.0023, Gamma=0.15, Delta=0.47, BA.2.12.1=0.0062, BA.2.75=0.016, BA.4/5=0.15, BA.1=0.91 *vs* Wuhan), with maximum efficiency for the variants BA.2.12.1 and BA.2.75, both descending from the widely circulated BA.2 lineage. There were no Omicron endotype

dropouts in contrast to the vaccination cohort not in continuous exposure, with an incidence of 7% (95% CI 2% - 19%)[5].

pH-dependent affinity is a new way to assess the dissociation constant of the epitope-paratope complex which typically has a half-life 0.5 – 2 hours and is difficult to directly measure accurately due to the instrument stability required over long time periods. However, pH-dependent affinity is used routinely in the elution of antibodies at pH 2.5-3.0 during affinity chromatography[23] suggesting the binding complex can be titrated as shown in Figure S3 for the proteins N, RBD, S(Wuhan), and S(Omicron) although the variation is complex and highly protein dependent. A linear correlation has been shown with the complex half-life and Affinity constant, K_D (pM) shown in Figures S4 and S5. Further, the physiological importance of lower pH is also relevant to the nasal mucosa[24], which at pH 5.5 – 6.5, is significantly lower than the pH of the serum and the buffers used for conventional affinity measurements. A nasal mucosal protection mechanism would require antibody complexes to be sufficiently numerous and stable to prevent attachment to the angiotensin-converting-enzyme-2 receptor, a parameter described here as the high-affinity concentration.

The teacher cohort has waning antibody concentration over time and will enter the 2022-2023 winter with 35% of the cohort already vulnerable to infection, Figure 3, increasing to 46% in a further 60 days and 66% within 120 days based on an antibody half-life of 60 days[25]. The presence of variant-optimised antibodies should provide members of the cohort with protection against the Omicron sub-variants, assuming there are sufficient antibodies in the nasal mucosa as proposed, based on a protective threshold of 3.4 mg/L [8]. The bivalent vaccines to Wuhan and Omicron variants will also provide renewed antigen exposure and potentially aid in producing high affinity antibodies for Omicron and its sub-variants.

Conclusions

The immunity profile for staff in the constant-exposure cohort shows significant antibody maturation to all SARS-CoV-2 variant spike proteins, notably to the prevalent Omicron variants. Approximately, 25% of the cohort have full, pan-variant protection whereas the remainder have higher-quality antibodies focused on the preceding wave variants. A smart-boosting programme focused on high-transmission groups, such as teachers and parents/guardians of school-age children, could significantly reduce the risk of high infection levels within the population during each wave, as the pandemic transitions to endemic. Furthermore, extensive and readily measured immunity profiles may highlight specific endotype vulnerability to infection, and may even provide insight into long COVID complications.

Acknowledgements

Professor Shaw's Research Group at Exeter University and Attomarker would like to thank the schoolteachers and staff who participated in this research project. The authors would like to thank Dr Jonathan Snicker for their guidance on the potential strategic and policy implications of the scientific findings.

Supplementary Data

Figures

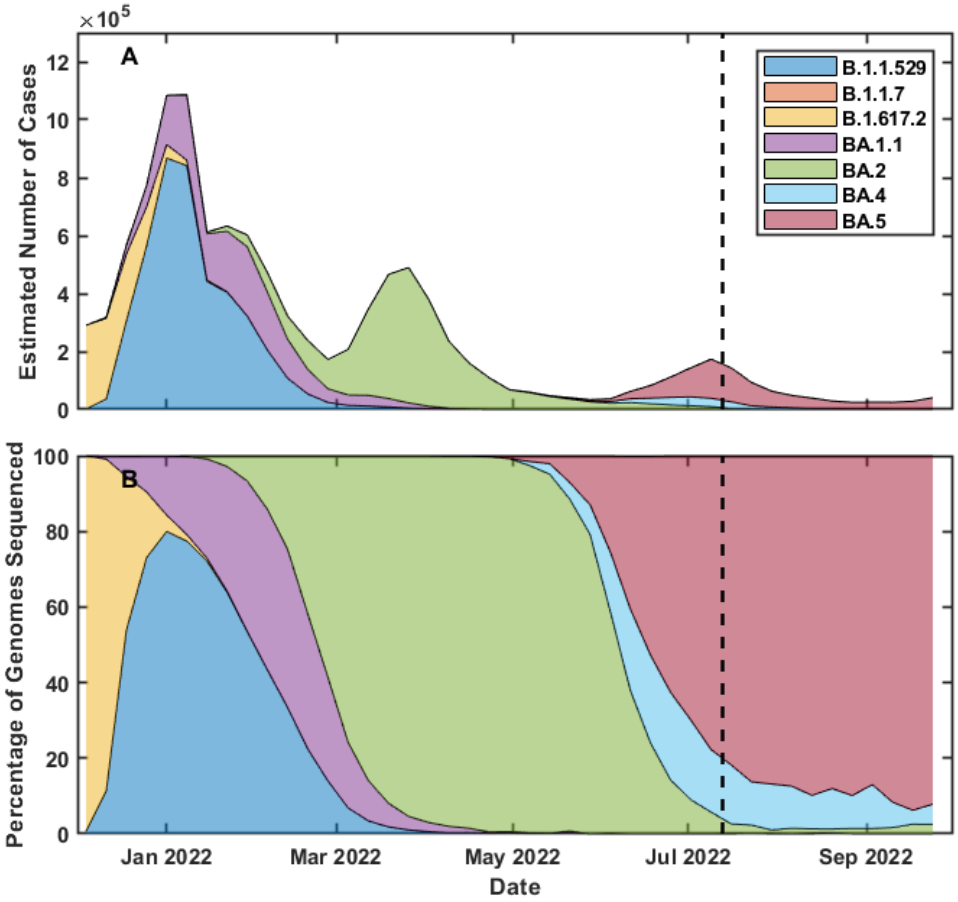

Figure S1 Prevalent SARS-CoV-2 variants preceding the cohort screen and the date of the cohort testing – shown using the black-dash line. Data is taken from the Wellcome Sanger Institute [26].

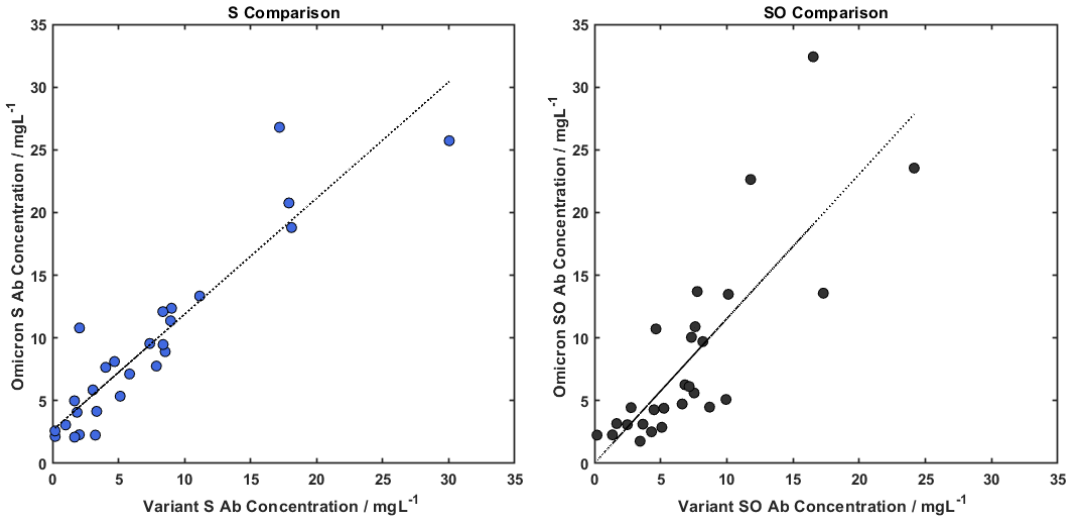

Figure S2. Correlation of Spike and Omicron Spike channels on the Variant and Omicron Sub-variant Arrays.

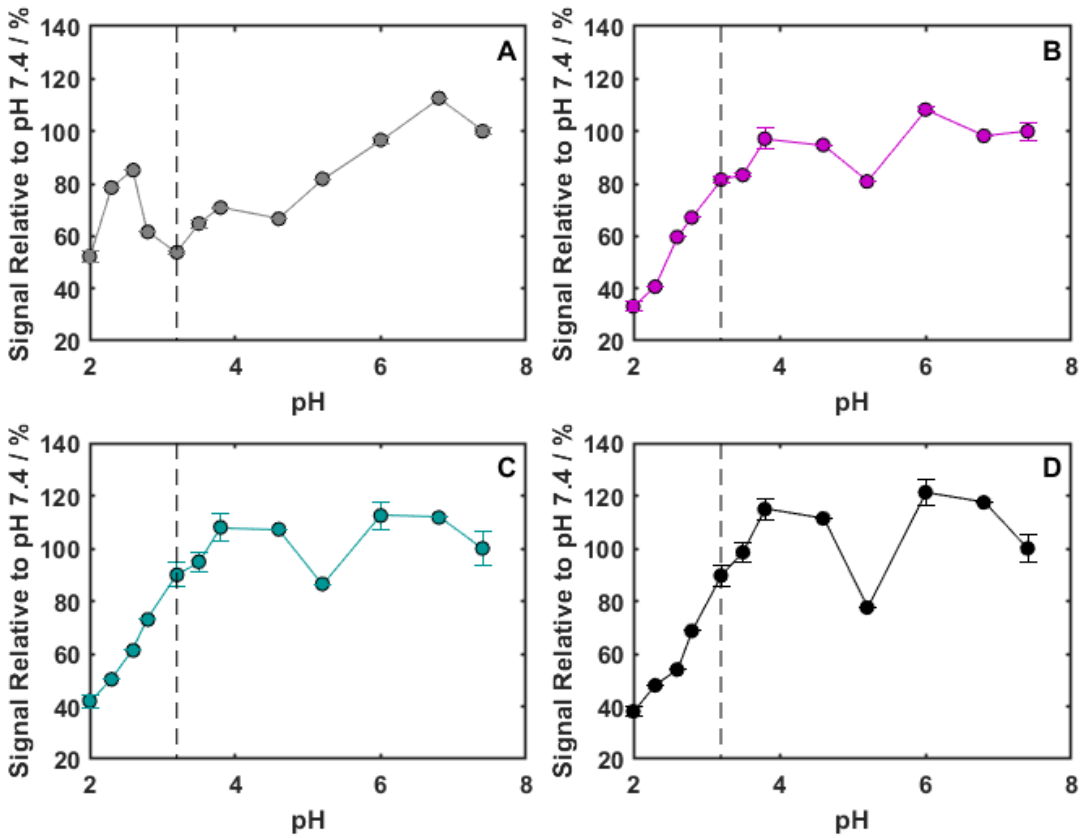

Figure S3 The change in concentration of the antibody assay with pH of an intermediate wash step. Protein Channels shown are the SARS-CoV-2 viral proteins: A) Nucleocapsid, B) RBD, C) S (Wuhan) and D) S (Omicron BA.1). Error bars show 1 SD. The vertical dotted line is drawn at pH 3.2.

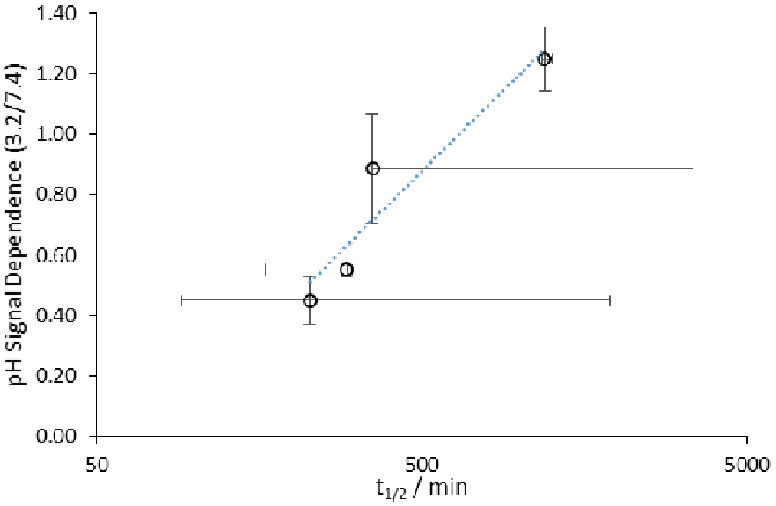

Figure S4 Plot of antibody-antigen half-life at pH 7.4 vs the pH dependence of the complex stability. Error bars show 1SD. The half-life was measured for four commercially sourced antibodies by recording the antibody dissociation over 20-30 minutes and fitting the data produced to a Langmuirian model. The pH dependence was determined by a sandwich assay with an intermediate wash step of 30s (between capture and detection) of varying pH.[ZHU1076 (Sigma-Aldrich), 40590-D001, 40590-T62 (Sinobiological), antiS2 1034617 (Biotechne)].

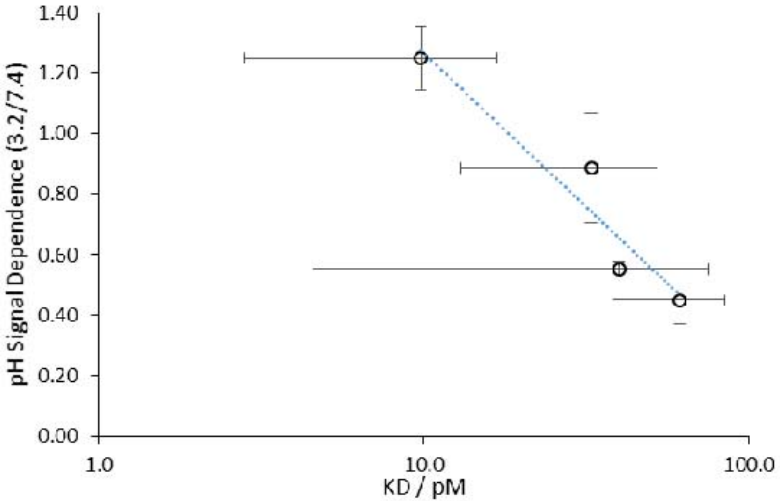

Figure S5 Plot of antibody K_D at pH 7.4 against the pH dependence of the complex stability. Error bars show 1 SD.

Tables

Table S1. The Spike proteins used to fabricate the Omicron Sub-variant test arrays.

Protein	Supplier	Cat #	Lot # (s)	Type	Cell Line	Tag	AA Length	Mutations
Wuhan	Sinobiological	40589-V08B1	MF16JU1612	Monomer	Baculovirus-Insect	C-term polyhistidine	1209	-
BA.1	Sinobiological	40589-V08H26	LC16JA1515	Trimer	HEK293	C-term polyhistidine	1228	A67V, HV69-70 deletion, T95I, G142D, VYY143-145 deletion, N211 deletion, L212I, ins214EPE, G339D, S371L, S373P, S375F, K417N, N440K, G446S, S477N, T478K, E484A, Q493R, G496S, Q498R, N501Y, Y505H, T547K, D614G, H655Y, N679K, P681H, N764K, D796Y, F817P, N856K, A892P, A899P, A942P, Q954H, N969K, L981F, K986P, V987P and furin cleavage site mutants
BA.2.12.1	Sinobiological	40589-V08H34	MB16JU1681	Trimer	HEK293	C-term polyhistidine	1228	T19I, L24S, del25-27, G142D, V213G, G339D, S371F, S373P, S375F, T376A, D405N, R408S, K417N, N440K, L452Q, S477N, T478K, E484A, Q493R, Q498R, N501Y, Y505H, D614G, H655Y, N679K, P681H, S704L, N764K, D796Y, A892P, A899P, A942P, Q954H, N969K, K986P, V987P and furin cleavage site mutants
BA.2.75	Acro Biosystems	SPN-C522f	6764A-227DF1-146	Trimer	HEK293	C-term polyhistidine	1197	.T19I, LPP24-26del, A27S, G142D, K147E, W152R, F157L, I210V, V213G, G257S, G339H, S371F, S373P, S375F, T376A, D405N, R408S, K417N, N440K, G446S, N460K, S477N, T478K, E484A, Q498R, N501Y, Y505H, D614G, H655Y, N679K, P681H, N764K, D796Y, Q954H, N969K, R683A, R685A, F817P, A892P, A899P, A942P, K986P,

								V987P. Proline substitutions (F817P, A892P, A899P, A942P, K986P, V987P) and alanine substitutions (R683A and R685A) are introduced to stabilize the trimeric prefusion state of SARS-CoV-2 S protein and abolish the furin cleavage site, respectively.
BA.4	Sinobiological	40589-V08H32	MB16JU1382	Trimer	HEK293	C-term polyhistidine	1226	F817P, A892P, A899P, A942P, K986P, V987P, T19I, L24del, P25del, P26del, A27S, H69del, V70del, G142D, V213G, G339D, S371F, S373P, S375F, T376A, D405N, R408S, K417N, N440K, L452R, S477N, T478K, E484A, F486V, Q498R, N501Y, Y505H, D614G, H655Y, N679K, P681H, N764K, D796Y, Q954H, N969K and furin cleavage site mutants
BA.5	Sinobiological	40589-V08H33	MB16JU1383	Trimer	HEK293	C-term polyhistidine	1226	F817P, A892P, A899P, A942P, K986P, V987P, T19I, L24del, P25del, P26del, A27S, H69del, V70del, G142D, V213G, G339D, S371F, S373P, S375F, T376A, D405N, K417N, N440K, L452R, S477N, T478K, E484A, F486V, Q498R, N501Y, Y505H, D614G, N679K, P681H, N764K, D796Y, Q954H, N969K and furin cleavage site mutants
Alpha	**Sinobiological**	**40589-V08B6**	**LC15MC0903**	**Monomer**	**Baculovirus-Insect**	**C-term polyhistidine**	**1206**	**HV69-70 deletion, Y144 deletion, N501Y, A570D, D614G, P681H, T716I, S982A, D1118H**
Beta	Sinobiological	40589-V08B7	LC15MY2607	Monomer	Baculovirus-Insect	C-term polyhistidine	1206	L18F, D80A, D215G, LAL242-244 deletion, R246I, K417N, E484K, N501Y, D614G, A701V

Gamma	Sinobiological	40589-V08B8	LC15JU0209	Monomer	Baculovirus-Insect	C-term polyhistidine	1209	L18F, T20N, P26S, D138Y, R190S, K417T, E484K, N501Y, D614G, H655Y, T1027I
Delta	Sinobiological	40589-V08B16	LC15OC2012	Monomer	Baculovirus-Insect	C-term polyhistidine	1207	T19R, G142D, E156G, HR157-158 deletion, L452R, T478K, D614G, P681R, D950N
Omicron	Sinobiological	40589-V08B33	MF15DE2961	Monomer	Baculovirus-Insect	C-term polyhistidine	1206	A67V, HV69-70del, T95I, G142D, VYY143-145del, N211del, L212I, ins214EPE, G339D, S371L, S373P, S375F, K417N, N440K, G446S, S477N, T478K, E484A, Q493R, G496S, Q498R, N501Y, Y505H, T547K, D614G, H655Y, N679K, P681H, N764K, D796Y, N856K, Q954H, N969K, L981F

Table S2. Gradient (m), intercept (c) and R^2 values for the correlation of similar channels on the Spike Variant Array and the Spike Omicron Array.

Protein Pair x/y	**Slope**	**Intercept**	**R^2**
S (monomer)/S (monomer)	0.93	2.6	0.92
SO (monomer) /SO (trimer)	1.15	0.0	0.81

Table S2. Endotype classification and symbols used to represent them.

Endotype	Symbol	Classification
Universal Negative	U(-)	All antibody concentrations are ≤LoD 0.2 mg/L
Universal Positive	U(+)	All antibody concentrations are > 2 mg/L (LoQ) and each concentration is >10% of the peak concentration (defined as the maximum concentration across all spike variants for that sample)
Dropout Endotypes	U(±)	
Single Dropout	*e.g.* W,α,β,γ,δ,ο (-)	A single antibody concentration is <10% of the peak concentration and that peak >2 mg/L
Double Dropout Subclasses	2(-) *e.g.* αβ(-)	Two antibody concentrations are <10% of the peak concentration and that peak >2 mg/L (LoQ)
Triple Dropout Subclasses	3(-) *e.g.* αβγ(-)	Three antibody concentrations are <10% of the peak concentration and that peak >2 mg/L (LoQ)
Quadruple Dropout Subclasses	4(-) *e.g.* αβγδ(-)	Four antibody concentrations are <10% of the peak concentration and that peak >2 mg/L (LoQ)
Quintuple Dropout Subclasses	5(-) *e.g.* αβγδο(-)	Five antibody concentrations are <10% of the peak concentration and that peak >2 mg/L (LoQ)
Unclassified	U(~)	All results are ≥0.2 mg/L (LoD), but not all >2 mg/L (LoQ). No large disparities in concentration between variants.

Table S3. Antibodies used for production of $t_{1/2}$ to k_d plot.

Ab	**Immunogen**	**SKU**	**Batch**	**Manufacturer**	**Type**
Clone hu2B3E5 ZooMAb	Recombinant S fragment from SARS-CoV	ZHU1076	Q3506110	Sigma Aldrich	Mouse/Human recombinant monoclonal
Spike S2 Antibody	Recombinant SARS-CoV-2 Spike S2 ECD (#40590-V08B)	40590-D001	HA14AP2901	Sinobiological	Rabbit/Human recombinant monoclonal
anti S2 1034617	Recombinant SARS-CoV2 Spike S2 Subunit	MAB10557-100	CNEF0121021	Biotechne	Mouse Monoclonal
Spike S2 Antibody	Recombinant SARS-CoV-2 Spike S2 ECD (#40590-	40590-T62	HD15JU0103	Sinobiological	Rabbit polyclonal

V08B)

Table S4 Additional cohort demographics.

Age	**16-24**	**25-34**	**35-44**	**45-54**	**55-64**	**65-74**	**75+**
%	4	14	14	21	32	11	4
Initial 2 Dose Vaccine	**AZ**	**Pfizer**	**Moderna**	**Unknown**			
%	68	25	4	4			

References

1. Burridge HC, Fan S, Jones RL, Noakes CJ, Linden PF. Predictive and retrospective modelling of airborne infection risk using monitored carbon dioxide. *Indoor and Built Environment* 2021; **31**(5): 1363-80.
2. Manica M, Poletti P, Deandrea S, et al. Estimating SARS-CoV-2 transmission in educational settings: A retrospective cohort study. *Influenza and Other Respiratory Viruses*; **n/a**(n/a).
3. Chudasama DY, Tessier E, Flannagan J, et al. Surge in SARS-CoV-2 transmission in school-aged children and household contacts, England, August to October 2021. *Euro surveillance : bulletin Europeen sur les maladies transmissibles = European communicable disease bulletin* 2021; **26**(48).
4. Flasche S, Edmunds WJ. The role of schools and school-aged children in SARS-CoV-2 transmission. *Lancet Infect Dis* 2021; **21**(3): 298-9.
5. James-Pemberton PH, Kohli S, Twynham J, et al. Fully Quantitative Measurements of Differential Antibody Binding to Spike Proteins from Wuhan, Alpha, Beta, Gamma, Delta and Omicron BA.1 variants of SARS-CoV-2: Antibody Immunity Endotypes. *medRxiv* 2022: 2022.09.23.22280271.
6. Formolo T LM, Levy M, Kilpatrick L, Lute S, Phinney K, et al. . Determination of the NISTmAb primary structure. State-of-the-Art and Emerging Technologies for Therapeutic Monoclonal Antibody Characterization: ACS Symposium Series; 2015: 1-62.
7. McLellan JS, Chen M, Kim A, Yang Y, Graham BS, Kwong PD. Structural basis of respiratory syncytial virus neutralization by motavizumab. *Nature structural & molecular biology* 2010; **17**(2): 248-50.
8. James-Pemberton PH, Helliwell MW, Olkhov RV, et al. Fully Quantitative Measurements of the Antibody Levels for SARS-CoV-2 Infections and Vaccinations calibrated against the NISTmAb Standard IgG Antibody. *medRxiv* 2022: 2022.07.12.22277533.
9. James-Pemberton P, Łapińska U, Helliwell M, et al. Accuracy and precision analysis for a biophotonic assay of C-reactive protein. *The Analyst* 2020: 10.1039/c9an02516b.
10. Shaw AM, Hyde C, Merrick B, et al. Real-world evaluation of a novel technology for quantitative simultaneous antibody detection against multiple SARS-CoV-2 antigens in a cohort of patients presenting with COVID-19 syndrome. *The Analyst* 2020.
11. James-Pemberton PH, Helliwell MW, Olkhov RV, et al. Vaccine, Booster and Natural Antibody Binding to SARS-CoV-2 Omicron (BA.1) Spike Protein and Vaccine Efficacy. *medRxiv* 2022: 2022.07.12.22277539.
12. Gurdasani D, Pagel C, McKee M, et al. Covid-19 in the UK: policy on children and schools. *BMJ (Clinical research ed)* 2022; **378**: e071234.
13. Pierce CA, Herold KC, Herold BC, et al. COVID-19 and children. *Science* 2022; **377**(6611): 1144-9.
14. WHO. Considerations for school-related public health measures in the context of COVID-19. 2020 (accessed 17th November 2022).
15. Röltgen K, Nielsen SCA, Silva O, et al. Immune imprinting, breadth of variant recognition, and germinal center response in human SARS-CoV-2 infection and vaccination. *Cell* 2022; **185**(6): 1025-40.e14.
16. Yu W, Zhong N, Li X, et al. Structure Based Affinity Maturation and Characterizing of SARS-CoV Antibody CR3022 against SARS-CoV-2 by Computational and Experimental Approaches. *Viruses* 2022; **14**(2).
17. Tang J, Grubbs G, Lee Y, et al. Antibody affinity maturation and cross-variant activity following SARS-CoV-2 mRNA vaccination: Impact of prior exposure and sex. *EBioMedicine* 2021; **74**: 103748.
18. Laidlaw BJ, Ellebedy AH. The germinal centre B cell response to SARS-CoV-2. *Nat Rev Immunol* 2022; **22**(1): 7-18.
19. Mishra AK, Mariuzza RA. Insights into the Structural Basis of Antibody Affinity Maturation from Next-Generation Sequencing. *Front Immunol* 2018; **9**: 117.
20. Victora GD, Nussenzweig MC. Germinal Centers. *Annu Rev Immunol* 2022; **40**: 413-42.
21. Tam HH, Melo MB, Kang M, et al. Sustained antigen availability during germinal center initiation enhances antibody responses to vaccination. *Proceedings of the National Academy of Sciences* 2016; **113**(43): E6639-E48.
22. McHeyzer-Williams LJ, McHeyzer-Williams MG. ANTIGEN-SPECIFIC MEMORY B CELL DEVELOPMENT. *Annual Review of Immunology* 2005; **23**(1): 487-513.
23. Ayyar BV, Arora S, Murphy C, O'Kennedy R. Affinity chromatography as a tool for antibody purification. *Methods* 2012; **56**(2): 116-29.
24. England RJ, Homer JJ, Knight LC, Ell SR. Nasal pH measurement: a reliable and repeatable parameter. *Clin Otolaryngol Allied Sci* 1999; **24**(1): 67-8.
25. Dan JM, Mateus J, Kato Y, et al. Immunological memory to SARS-CoV-2 assessed for up to 8 months after infection. *Science* 2021; **371**(6529): eabf4063.
26. COVID-19 Genomic Surveillance. 2022. https://covid19.sanger.ac.uk/lineages/raw?latitude=51.622741&longitude=-1.455710&zoom=4.708800&p_type=area&cases_type=area&xMin=2021-12-04&xMax=2022-09-24 (accessed 24/09/2022 2022).